

Supplementary Information for

**On-demand quantitative SERS bioassays facilitated by
surface-tethered ratiometric probes**

Kun Zhang^a, Yuning Wang^a, Meiling Wu^b, Yujie Liu^a, Dongyun Shib^a, and Baohong Liu^{*,a}

^a Department of Chemistry, Shanghai Stomatological Hospital, State Key Laboratory of Molecular Engineering of Polymers, Institutes of Biomedical Sciences, and Collaborative Innovation Center of Chemistry for Energy Materials Fudan University, Shanghai 200438, China

^b Department of Biochemistry and Molecular Biology, Shanghai Medical College of Fudan University, Shanghai 200032, China

*Correspondence to: bhliu@fudan.edu.cn

Supplementary Information

Table of Contents

S1. Materials and Instrumentation

S1.1 Reagents and Materials.

S1.2 Apparatus and Characterization

S2. Experimental Sections

S2.1 Synthesis of Citrate Stabilized-Gold Nanoparticles (GNPs).

S2.2 Fabrication of plasmonic Chips with immobilized Raman probes.

S2.3 Cell Culture

S2.4 SERS Quantification of H_2O_2

S2.5 SERS Quantification of Metabolites

S3. Additional Figures and Discussions

S3.1 Characterization of GNPs

S3.2 Preparation of SERS-active chips

S3.3 Estimation of Enhancement Factor

S3.4 Detection of H_2O_2

S3.5 Reproducibility and Stability

S3.6 Specificity of Glucose Detection

S3.7 Utilization of other probes

S1. Materials and Instrumentation

S1.1 Reagents and Materials. Chloroauric acid hydrate ($\text{HAuCl}_4 \cdot 4\text{H}_2\text{O}$, $\geq 47.8\%$ Au), trisodium citrate dihydrate ($\text{C}_6\text{H}_5\text{Na}_3\text{O}_7 \cdot 2\text{H}_2\text{O}$, $\geq 99\%$), sodium nitrite (NaNO_2 , $\geq 99\%$), ethanol ($\geq 99.7\%$), acetone ($\geq 99.5\%$), ammonia (25%), hydrogen peroxide (H_2O_2 , $\geq 30\%$), glucose ($\geq 99\%$), and sodium hypochlorite solution (NaOCl , 10%-15% available chlorine) were purchased from Sinopharm Chemical Reagent Co., Ltd (Shanghai, China). 3-Mercaptophenylboronic acid (3-MPBA, 95%), 3-hydroxythiophenol (3-HTP, 96%), cholesterol (99%), and sodium lactate (98%) were obtained from Aladdin Reagent Co., Ltd. (Shanghai, China). 3-Aminopropyl trimethoxysilane (APTMS, 97%) and 4-mercaptophenylboronic acid (4-MPBA, 95%) were obtained from Sigma-Aldrich. Glucose oxidase, cholesterol oxidase, and lactate oxidase were purchased from Shanghai Yuanye Bio-Technology Co., Ltd. (Shanghai, China). In the H_2O_2 selectivity test, Nitric oxide (NO) was obtained by slowly dropping H_2SO_4 (6 M) into a glass flask containing saturated NaNO_2 solution. Hydroxyl radical ($\cdot\text{OH}$) was generated by the Fenton reaction ($\text{Fe}^{2+}/\text{H}_2\text{O}_2 = 1:6$). All enzymatic reactions were performed in phosphate buffer (pH 7.4, 10 mM) unless otherwise mentioned. All chemicals were used without further purification. Ultrapure water ($>18.0 \text{ M}\Omega \cdot \text{cm}$) was obtained from a Millipore water system.

S1.2 Apparatus and Characterization

General Characterization. Ultraviolet-visible (UV-vis) extinction spectrum was determined on a UV-8000A UV-vis spectrophotometer (Shanghai Yuanxi, Shanghai, China). Transmission electron microscopic (TEM) images were obtained on a Tecnai G 2F20 S-TWIN transmission electron microscope (FEI, USA) at an accelerating voltage of 200 kV. Scanning electron microscopic (SEM) measurements were performed on a Nova NanoSEM 450 system (FEI, USA) at an accelerating voltage of 3 kV.

Raman Measurements. All Raman measurements were carried out on a Horiba XploRA confocal microscopic Raman spectrometer equipped with a 50 \times Olympus S2

objective lens (NA 0.55) and a 1200 grooves/mm grating were used (HORIBA Jobin Yvon, France). The powers of the 532 nm, 638 nm, and 785 nm lasers used to excite the samples were set to be 2.5 mW, 2.4 mW, and 9 mW, respectively. Each Raman spectrum was recorded in a range of 300~1800 cm^{-1} with an integration time of 10 s if it was not specified. The 520 cm^{-1} peak of silica was used to correct the grating before detection.

S2. Experimental Sections

S2.1 Synthesis of Citrate Stabilized-Gold Nanoparticles (GNPs). Citrate stabilized-GNPs were prepared in aqueous phase according to the classical Fren's method, that is the reduction HAuCl_4 by citrate.^[1] Briefly, 50 mL of HAuCl_4 solution (0.1% by weight) was heated to boiling, followed by the addition of 0.5 mL of citrate solution (1% by weight) under strong stirring. Then, the reaction mixture was refluxed for another 15 min to complete the reduction reaction. After cooling to room temperature, the as-prepared GNPs were subjected to TEM and UV-vis spectroscopic characterizations.

S2.2 Fabrication of plasmonic Chips with immobilized Raman probes. The SERS-active substrates were prepared by assembly of GNPs on the surfaces of indium tin oxide (ITO) glass slides (3 mm \times 3 mm).^[2,3] Before preparation, the ITO slides were first cleaned by sonicating in acetone, ethanol, and water for 15 min, respectively, followed by immersing in a mixture solution of water, H_2O_2 (30%) and ammonia (5:1:1, v/v) for 30 min. After rinsing with large amounts of water and drying in nitrogen, the slides were immersed in 1% (v/v) APTMS ethanol solution for 30 min, washed three times with ethanol and further sonicated in ethanol for 5 min to remove the loosely bound APTMS molecules. Finally, the slides were annealed at 120 $^{\circ}\text{C}$ for 3 hours to complete the silanization modification. To form a self-assembled monolayer of GNPs on the ITO surface, the amino functionalized slides were immersed into the GNP dispersion for 24 h followed by rinsing with water and drying in air. The Raman probes were immobilized on the plasmonic substrates via the S-Au covalent interaction. For the immobilization of 3-MPBA, the slides were immersed in 1 mM of the 3-MPBA

ethanol solution for 24 h followed by washing with ethanol and dry in nitrogen. For the assembly of other probes, the same procedure was employed excepted for the probe solution.

S2.3 Cell Culture. The A549, HepG2 and LO2 cell lines were obtained from the Cell Bank of the Chinese Academy of Sciences (Shanghai, China). Cells were cultured in Dulbecco's modified Eagle's medium (DMEM, Gibco, USA) with supplemented with 10% fetal bovine serum (FBS, Gibco, USA), penicillin and streptomycin, and were maintained in a humidified 37°C a humidified incubator (Forma Scientific) with an atmosphere containing 5% CO₂. For glucose limitation experiments, cells were cultured in glucose- and glutamine-free DMEM supplemented with 10% FBS, and glutamine (2 mM) or glucose (25 mM) was added as required. For all three types of cell lines, cells were plated in 6-well plates (approximately 5×10^5 cells per well) for growth, and the cell number was determined by nucleus counting before collection of the culture medium.

S2.4 SERS Quantification of H₂O₂. 5 μ L of H₂O₂ aqueous solution with concentrations from 0 to 500 nM was deposited on the 3-MPBA-functionalized chip surface and incubated at r.t. for 20 min. The SERS responses were then measured after washing the chip with water and drying in nitrogen.

S2.5 SERS Quantification of Metabolites. For glucose sensing, 5 μ L, 50 μ g/mL of glucose oxidase in phosphate buffer solution (10 mM, pH 7.0) was incubated with 15 μ L of glucose standard solution or cellular culture matrix at 37 °C for 30 min. Then, 10 μ L of the reaction mixture was pipetted onto the plasmonic chip and incubated for 20 min followed by scanning the SERS spectra. For the detection of lactate or cholesterol, 10 μ g/mL of lactate oxidase or cholesterol oxidase was used, respectively.

S3. Additional Figures and Discussions

S3.1 Characterization of GNPs

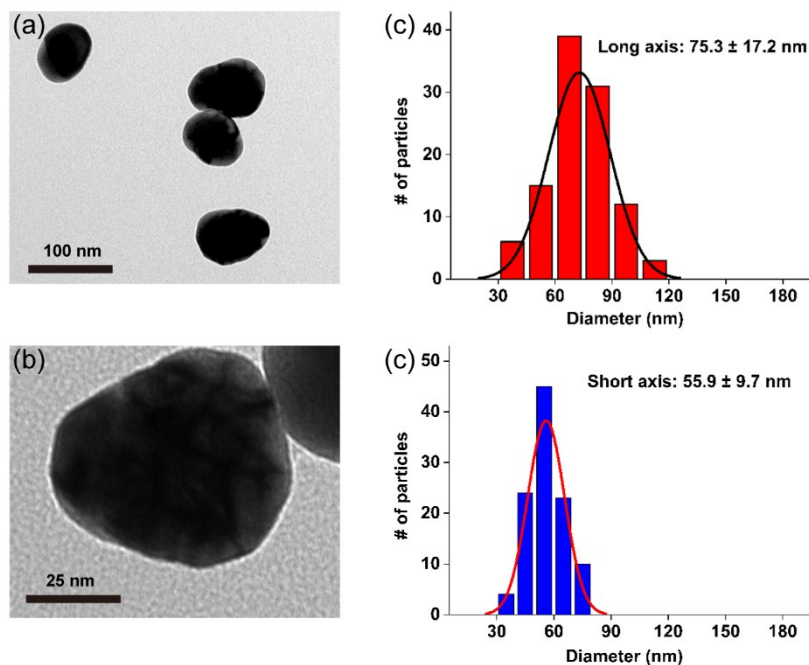


Fig. S1. Characterization of GNPs. (a) and (b) TEM images of citrate-stabilized GNPs. Size distribution of GNPs estimated according to the length of (c) the long axis and (d) the short axis.

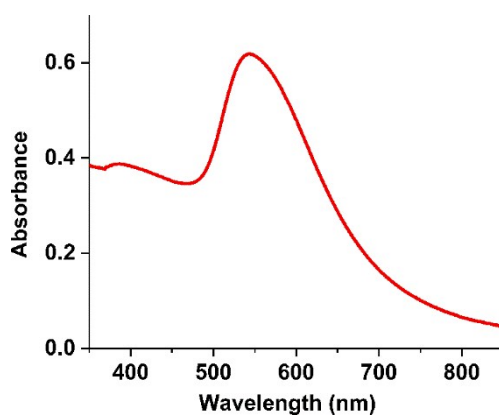


Fig. S2. UV-vis extinction spectrum of the GNP colloidal solution in water. The typical localized surface plasmon resonance peak was at around 542 nm.

We choose GNPs as the building blocks to fabricate the SERS-active substrates because of their strong plasmonic resonance and good chemical stability.^[4] As depicted in

Figure S1, the synthesized GNPs exhibit an ellipsoidal structure. The average size estimated from the long axis is ca. 75.3 ± 17.2 nm, 20 nm larger than that calculated from the short axis. Such an irregular appearance combined with the relative large polydispersity indicates that there exists an apparent structural heterogeneity among different GNPs. This is also revealed by the broadened extinction spectrum of gold colloids (Figure S2).

S3.2 Preparation of SERS-active chips

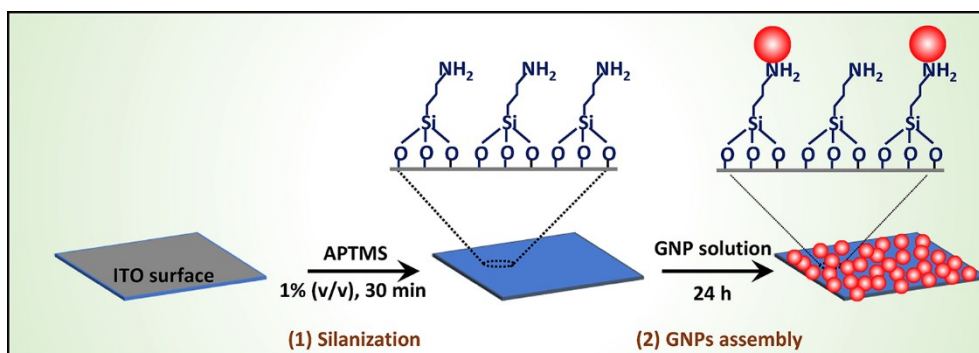


Fig. S3. Schematic illustration showing the preparation of SERS chips by assembling citrated-stabilized GNPs on amine-modified ITO slides via the electrostatic interaction.

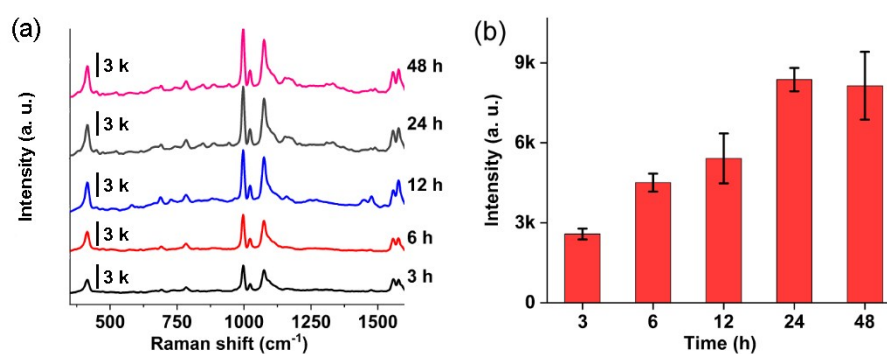


Fig. S4. Optimization of Au NP assembly time. (a) SERS responses of Au chips formed by immersing ITO slides in 30 nm GNPs for 3 h, 6 h, 12 h, 24 h and 48 h, respectively. 3-MPBA densely adsorbed on the formed Au chip was used as a Raman reporter. (b) Histogram of SERS intensities (I_{998}) of the spectra in (a). The error bars indicate the standard deviations of the three repeated measurement.

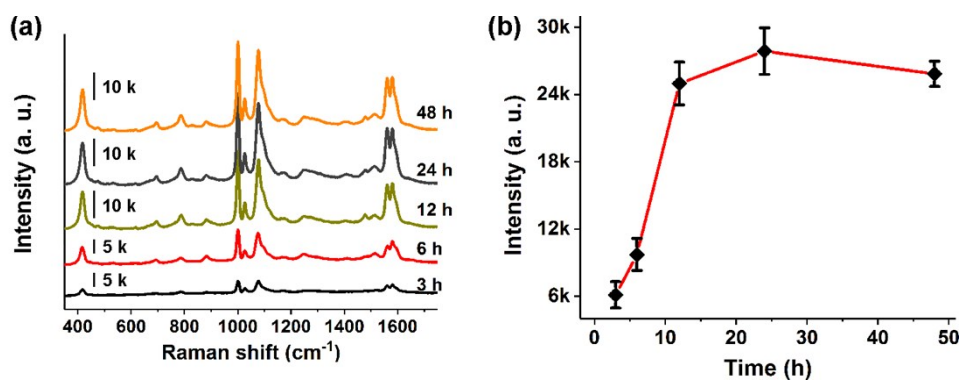


Fig. S5. Optimization of probe adsorption time. (a) SERS spectra of 3-MPBA immobilized on Au chips for 3 h, 6 h, 12 h, 24 h and 48 h, respectively. (b) Histogram of the SERS intensities (I_{998}) of the spectra in (a). The error bars indicate the standard deviations of the three repeated measurements.

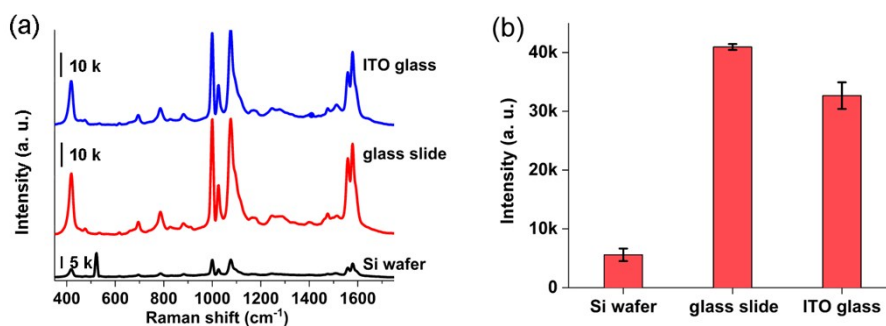


Fig. S6. Optimization of substrates. (a) SERS responses of Au chips formed by assembling GNPs on different substrate surfaces (Si wafer, glass slide, and ITO glass). 3-MPBA densely adsorbed on the formed Au chip was used as a Raman reporter. (b) Histogram of SERS intensities (I_{998}) of the spectra in (a). The error bars indicate the standard deviations of the three repeated measurements.

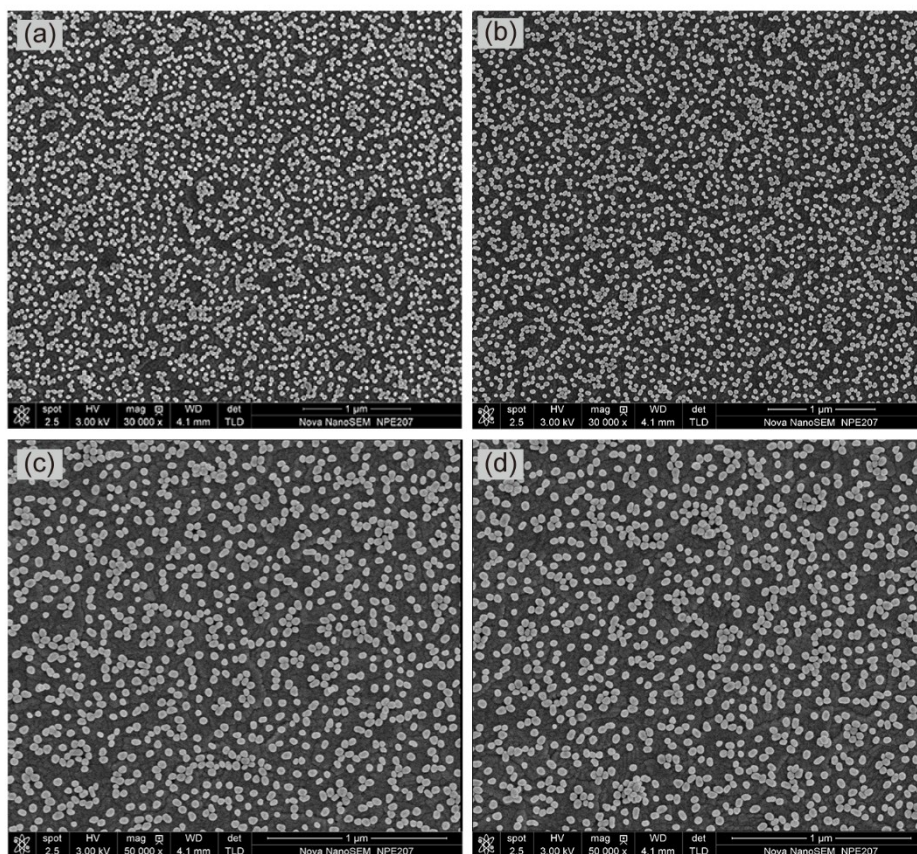


Fig. S7. SEM images of SERS chips showing disordered distribution of GNPs on the surface of the ITO slide.

We prepared the plasmonic substrates by electrostatic adsorption of the citrate-stabilized GNPs on the amino-functionalized ITO surfaces. This is a simple and classical technique capable of producing batches of dense GNP monolayers on the surfaces of solid substrates. Here we choose the ITO coated glass slide as the supporting matrix not only because of its ease of aminosilylation, but also because of its good conductivity that allows robust tracking of the chip fabrication process. We estimated the surface coverage of GNPs on the ITO surface by using ImageJ software. For the two chips depicted in Figure S7a and S7b, the surface densities of GNPs are 31.6% and 31.1%, respectively, implying that there is no apparent difference in the amounts of probes adsorbed on different chips. However, due to the disordered arrangement of GNPs and the heterogeneous particle structure, upon laser excitation, the largely enhanced local electric fields (hot spots) are inevitably exhibit an inhomogeneous

distribution at the chip surface, leading to intense fluctuations among point-to-point SERS responses and the deviation in accuracy of the measurement especially then the small laser spot size is used.^[5]

S3.3 Estimation of Enhancement Factor

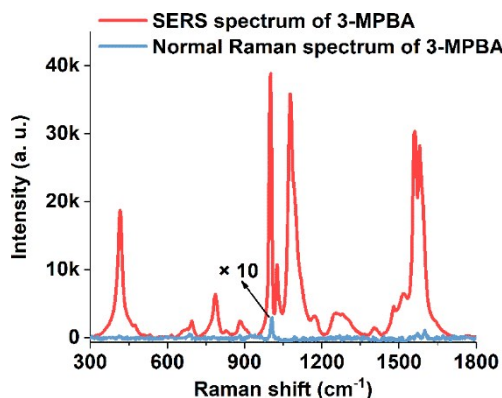


Fig. S8. Comparison between SERS spectrum (red line) of 3-MPBA recorded from the Au chip and Normal Raman spectrum (blue line) of 3-MPBA solution (0.5 M).

With reference to the 998 cm⁻¹ SERS band of 3-MPBA, we calculate the enhancement factor (EF) as followed:^[6]

$$EF = (I_{SERS}/N_{SERS})/(I_{Raman}/N_{Raman}) \quad (S1)$$

where N_{SERS} and N_{Raman} represent the numbers of 3-MPBA molecules measured using the SERS chip and normal Raman, respectively. I_{SERS} and I_{Raman} are the signal intensities measured using SERS and normal Raman, respectively. To perform both SERS and Raman measurements under identical experimental conditions, we use a 638 nm laser ($P = 0.24$ mW) to excite the sample, and an Olympus 10× objective lens ($NA = 0.25$) to collect the Raman photons. The integration time is set to 10 s per spectrum. On the basis of the TEM results, the GNPs are assumed to be ellipsoids, having the major and minor axis radii of 37.5 nm and 28 nm, respectively. The numbers of GNPs within the focused laser spot is calculated as followed:

$$N_{GNP} = 0.31 \times S_{laser}/S_{GNP} \quad (S2)$$

where S_{laser} is the area of the focused laser spot. S_{GNP} ($3.3 \times 10^3 \text{ nm}^2$) is the cross-sectional area of a single GNP. 0.31 is the coverage of GNPs at the chip surface.

S_{laser} can be calculated by formula (S3):

$$S_{\text{laser}} = \pi d^2/4 = \pi(1.22\lambda/\text{NA})^2/4 = 7.61 \times 10^6 \text{ nm}^2 \quad (\text{S3})$$

Thus, the GNP number (N_{GNP}) within the laser spot is estimated to be 715, which is ca. 3.2-fold larger than that obtained from the TEM images, meaning that the actual obtained EF may be three times lower. The van der Waals dimension of the 3-MPBA molecule is assumed to be $0.4 \text{ nm} \times 0.7 \text{ nm}$.^[7] Considering nonideal packing, surface defects, and steric constraints, the surface occupied by each probe molecule should be increased. Therefore, the specific surface of ATP molecules is approximated to be 1 nm^2 . For demonstration purpose, this approximation is quite acceptable, but the calculated EF value would be triple down again. According to this assumption, the number of 3-MBA (N_{SERS}) within the focused laser spot is 2.36×10^6 .

For normal Raman determination, we use a glass capillary ($D_{\text{inner}} = 0.5 \text{ mm}$) to load the sample. The focal plane of the laser irradiation is at the center section of the capillary. The sampling volume is thus calculated as followed:

$$V = Sh = 7.61 \times 10^6 \text{ nm}^2 \times 2.5 \times 10^5 \text{ nm} = 1.9 \times 10^{12} \text{ nm}^3 \quad (\text{S4})$$

The number of 3-MPBA (N_{Raman}) is calculated as followed:

$$N_{\text{Raman}} = 6.02 \times 10^{23} \times 0.5 \text{ M} \times 1.9 \times 10^{12} \text{ nm}^3 = 5.72 \times 10^{11} \quad (\text{S5})$$

Finally, according to formula (S1), we calculate the EF value of ca. 2.4×10^7

S3.4 Detection of H₂O₂

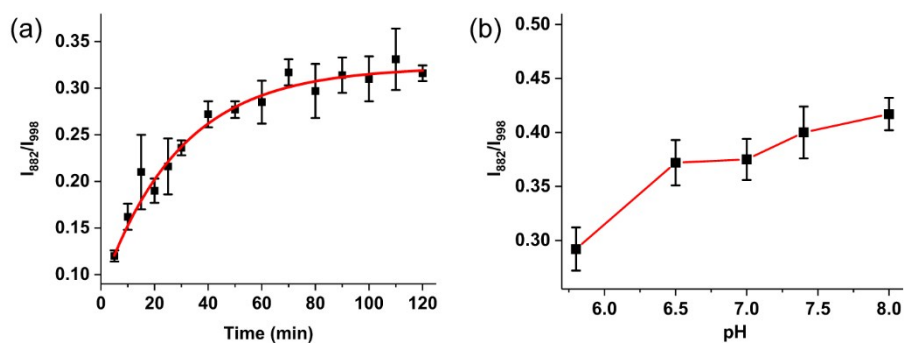


Fig. S9. Optimization of reaction conditions for H₂O₂ detection. (a) Ratiometric SERS intensities versus reaction time based on I_{882}/I_{998} . (b) Ratiometric SERS intensities versus buffer pH based on I_{882}/I_{998} .

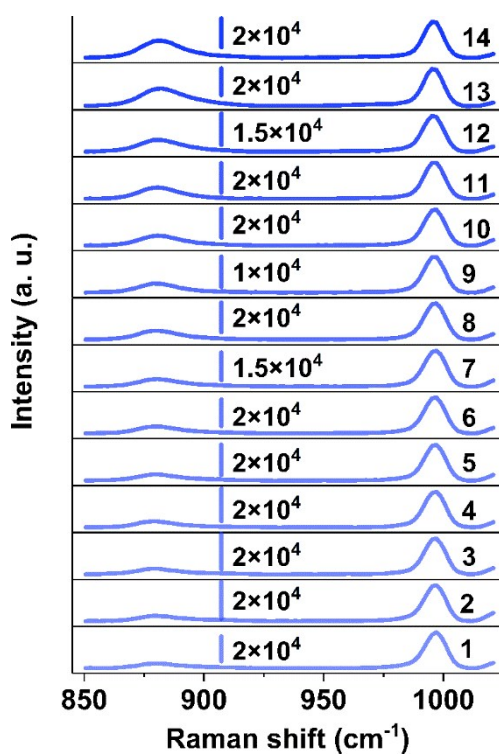


Fig. S10. SERS spectra of 3-MPBA as a function of H₂O₂ concentration (1 to 14: 50 nM, 100 nM, 250 nM, 500 nM, 1 μM, 5 μM, 25 μM, 50 μM, 100 μM, 250 μM, 500 μM, 1 mM, 5 mM, and 10 mM).

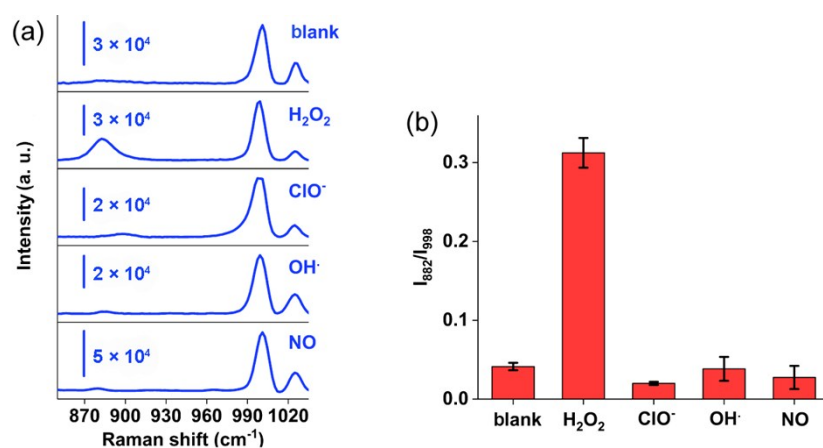


Fig. S11. Specificity test of ratiometric SERS for H_2O_2 detection. (a) SERS spectra of 3-MPBA immobilized on an Au chip in the presence of H_2O_2 (0.5 mM) against other reactive oxygen species (0.5 mM). (b) Histogram of the SERS intensity ratios (I_{882}/I_{998}) of the spectra in (a). The error bars indicate the standard deviations of the three repeated measurements.

S3.5 Reproducibility and Stability

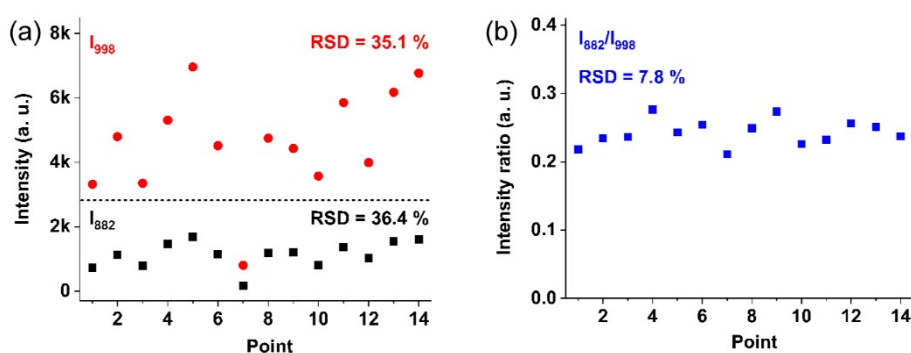


Fig. S12. Intra-chip reproducibility improvement test. The integration time is 2 s.

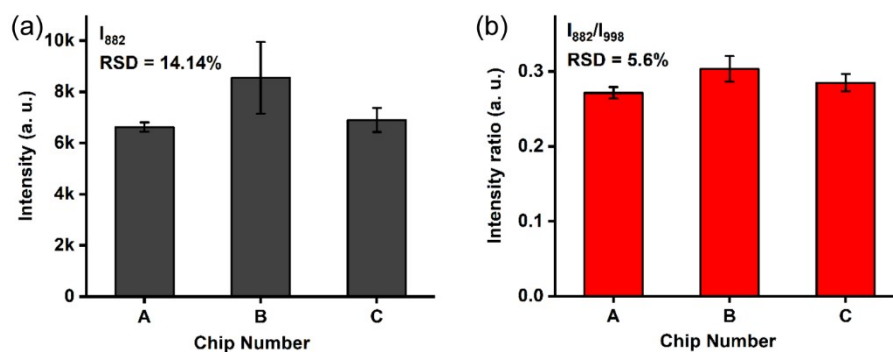


Figure S13. Inter-chip reproducibility improvement. The integration time is 2 s.

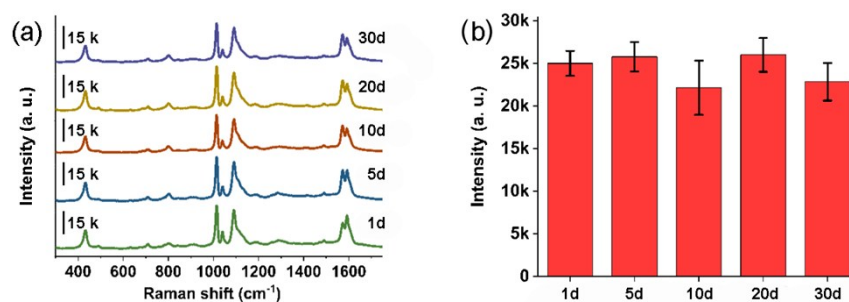


Fig. S14. Long time stability test for the Au chip. (a) SERS spectra acquired from the chip surface after different storage time. 3-MPBA densely adsorbed on the chip surface was used as SERS reporter. (b) Histogram of SERS intensities (I_{998}) of the spectra in (a). The error bars indicate the standard deviations of the three repeated measurements.

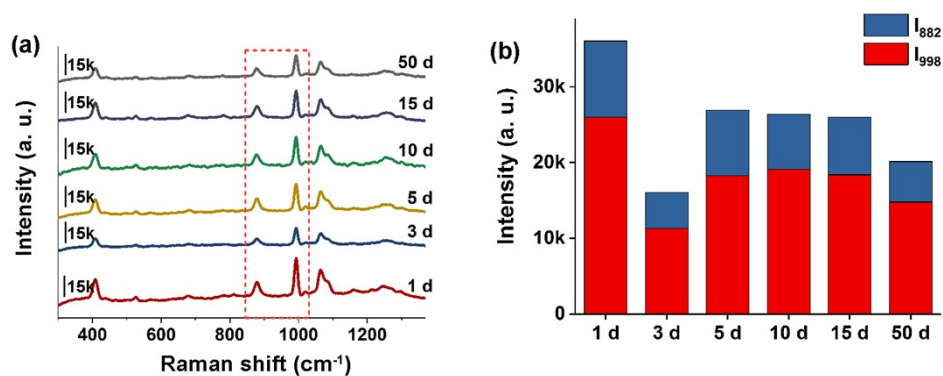


Fig. S15. Signal stability test for the Au chip after H₂O₂ detection. (a) SERS spectra determined after different storage time. (b) Histogram of SERS intensities of the 882 cm⁻¹ and 998 cm⁻¹ bands of the spectra in (a)

S3.6 Specificity of Glucose Detection

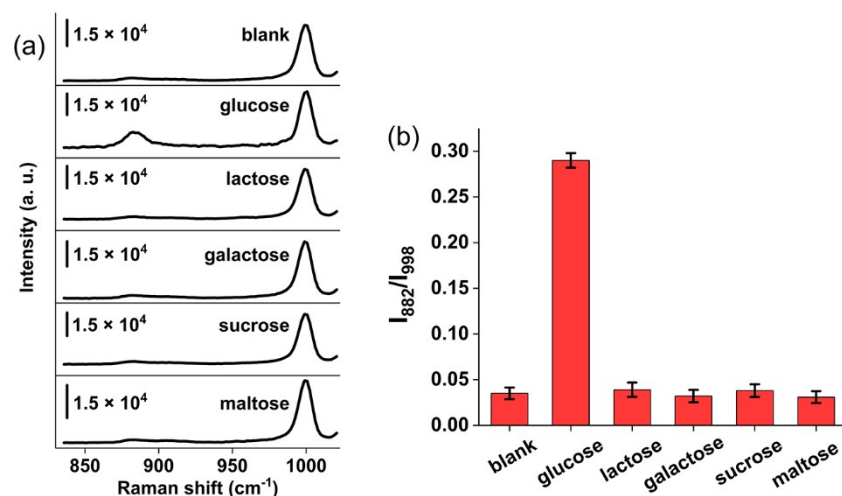


Fig. S16. Specificity test of ratiometric SERS for glucose detection. (a) SERS spectra of 3-MPBA immobilized on an Au chip in the presence of glucose against other sugars (50 mM). (b) Histogram of the SERS intensity ratios (I_{882}/I_{998}) of the spectra in (a). The error bars indicate the standard deviations of the three repeated measurements. Thanks to the specific recognition of oxidase to its substrate, such as the detection of glucose by glucose oxidase shown above, the good selectivity is guaranteed.

S3.7 Utilization of other probes

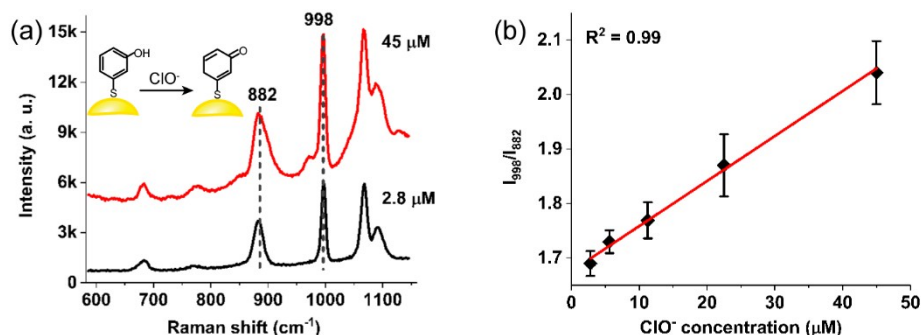


Fig. S17. Quantitative SERS detection of ClO^- using 3-HTP as a ratiometric probe immobilized on the Au chip surface. (a) SERS spectra of 3-HTP in the presence of 2.8 and 45 μM of ClO^- . (b) Linear plot of the SERS intensity ratios (I_{998}/I_{882}) against ClO^- concentrations ranging from 2.8 to 45 μM . The error bars indicate the standard deviations of the three repeated measurements.

The hydroxybenzene group of 3-HTP was converted into a quinonyl group in the presence of hypochlorite, accompanied by the decrease of the peak intensity at 882 cm^{-1} , and together with a little change of the peak at 998 cm^{-1} .^[8]

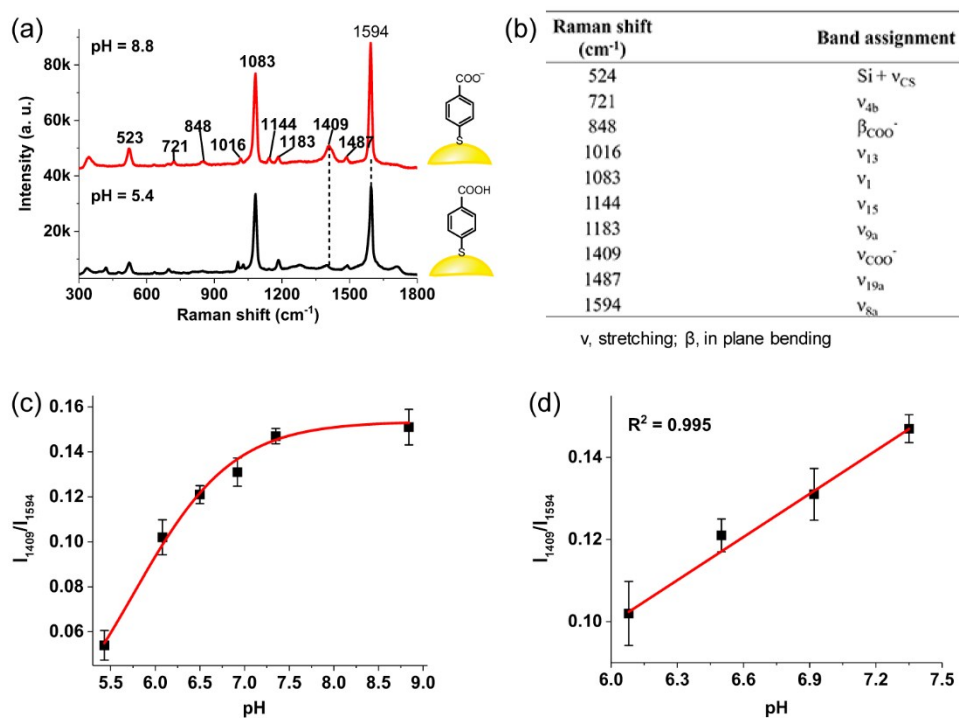


Fig. S18. Quantitative SERS detection of pH variations using 4-MBA as a ratiometric probe immobilized on the Au chip surface. (a) SERS spectra of 4-MBA under pH 5.4 and pH 8.8. (b) The assignment of SERS vibrational frequencies for 4-MBA. (c) Ratiometric SERS intensities versus pH concentration based on I_{1409}/I_{1594} . (d) Linear plot of the SERS intensity ratios (I_{1409}/I_{1589}) against pH values ranging from 6.1 to 7.4. The error bars indicate the standard deviations of the three repeated measurements.

References

- 1 G. Frens, *Nat. Phys.*, 1973, **241**, 20-22.
- 2 M.-D. Li, Y. Cui, M.-X. Gao, J. Luo, B. Ren and Z.-Q. Tian, *Anal. Chem.*, 2008, **80**, 5118-5125.
- 3 H. Cha, J. H. Yoon and S. Yoon, *ACS Nano*, 2014, **8**, 8554-8563.
- 4 W. Zhou, X. Gao, D. Liu and X. Chen, *Chem. Rev.*, 2015, **115**, 10575-10636.
- 5 A. C. Crawford, A. Skuratovsky and M. D. Porter, *Anal. Chem.*, 2016, **88**, 6515-6522.
- 6 E. C. Le Ru, E. Blackie, M. Meyer and P. G. Etchegoin, *J. Phys. Chem. C*, 2007, **111**, 13794-13803.
- 7 B. N. Khlebtsov, V. A. Khanadeev, E. V. Panfilova, D. N. Bratashov and N. G. Khlebtsov, *ACS Appl. Mater. Interfaces*, 2015, **7**, 6518-6529.
- 8 W. Wang, L. Zhang, L. Li, and Y. Tian, *Anal. Chem.*, 2016, **88**, 9518-9523.